Langmuir

Article

Graphene-Induced Self-Assembly of Peptides into Macroscopic-Scale Organized Nanowire Arrays for Electrochemical NADH Sensing

Panpan Li, Xu Chen, and Wensheng Yang

Langmuir, **Just Accepted Manuscript** • DOI: 10.1021/la401881a • Publication Date (Web): 20 Jun 2013

Graphene-Induced Self-Assembly of Peptides into Macroscopic-Scale Organized Nanowire Arrays for Electrochemical NADH Sensing

Panpan Li, Xu Chen, and Wensheng Yang**

State Key Laboratory of Chemical Resource Engineering, Beijing University of Chemical Technology, Beijing 100029 (P.R. China)

ABSTRACT: Controlling the macroscopic organization of self-assembled peptide nanostructures on a solid surface is a key challenge in enabling their technological applications. Here, we report a simple approach to achieve the horizontally organized self-assembly of dipeptides by introducing graphene sheets. We show at the first time the formation of a macroscopic-scale, high-density and ordered interlaced array of peptide nanowires and graphene composite (PNWs-G) on a silicon surface under mild conditions. The action of graphene sheets in the formation of the organized bionanostructure was preliminarily investigated. Furthermore, due to the introduction of graphene, the electronic conductivity of the bionanostructures was greatly improved, which is very beneficial for their applications in bioelectrochemical and nanoelectronic devices. As an applied example, the significantly enhanced electrochemical sensing performance for dihydronicotinamide adenine dinucleotide (NADH) was also demonstrated at the PNWs-G modified electrode relative to the alone component and unordered composite modified electrodes. The simple and mild approach described here opens a new avenue for the fabrication of macroscopic-scale organized self-assembled peptide bionanostructures on a solid surface, which should be capable of being extended to other biosystems based on graphite surface-template assembly, allowing a variety of functional bionanostructures to be fabricated and used in practical applications.

INTRODUCTION

The nanostructures fabricated from peptide building blocks are extremely attractive for bionanotechnology applications owing to their biocompatibility, chemical versatility, biological recognition and facile synthesis.[1–3] Recently the simplest peptide building blocks such as the diphenylalanine (FF) motif of the Alzheimer's β-amyloid peptide have received increasing attention.[4–7] Self-assembled FF-based nanostructures, especially peptide nanotubes (PNTs), have extraordinary mechanical strength and good chemical and thermal stability,[8,9] which make them appealing structural elements for various applications.[10–12] However, in developing novel uses for peptide nanostructures, controlling their macroscopic organization or alignment on a solid surface is needed,[13] which remains a significant challenge.

A major obstacle to realize the aim involves in the complexity of current 'solution-based' approaches to peptide nanofabrication, which caused dispersion and agglomeration problems.[14,15] Hence the solid-phase growth method of crystalline peptide nanostructures, such as a high-temperature aniline vapor aging method[14] and vapour deposition methods,[16] have been presented and vertically well-aligned arrays of PNTs have been successfully fabricated by using these methods. However, both methods involved high temperature process and organic vapors were also used in the former method. Magnetic field inducement[17] and inkjet printing technology[18] have been also tried to form the horizontal array of PNTs. Nevertheless the dense and ordered array of horizontal PNTs on a large scale has not been realized yet. Therefore, developing a simple and mild method for the fabrication of large and organized arrays of PNTs on a solid surface is highly desirable in the practical applications of PNTs.

In the present study, we report a simple approach to achieve the horizontally organized self-assembly of FF by introducing graphene sheets. For the first time, a high-density and

macroscopic-scale organized array of peptide nanowires and graphene composite (PNWs-G) was successfully fabricated on the surface of a silicon substrate under mild conditions. The action of graphene sheets in the formation of the organized bionanostructure was preliminarily investigated. In addition, the PNWs-G array showed good electronic conductivity due to the introduction of graphene sheets and its further application in the electrochemical sensor of NADH was also demonstrated.

EXPERIMENTAL SECTION

Chemicals. Diphenylalanine (FF) peptide in a lyophilized form was obtained from Bachem (Bubendorf, Switzerland). 1,1,1,3,3,3-Hexafluoro-2-propanol (HFIP) was purchased from Aladdin Chemicals Co. Ltd., China. Graphite powder (99.9%, 325 mesh) was obtained from Alfa Aesar. Hydrazine hydrate (80 wt.%) and ammonia solution (25 wt.%) were provided by Beijing Chemicals Inc. (Beijing, China). All aqueous solutions were prepared with deionized, doubly distilled water.

Preparation of Graphene Sheets. Graphite oxide (GO) was prepared from graphite powder according to a modified Hummers method.[19] The as-prepared GO sheets were then dispersed in water and exfoliated by ultrasonication for 2 h to form a stable dispersion. Hydrazine was used as the reductant to prepare the chemically reduced graphene sheets, as previously reported.[20] A homogeneous GO solution (0.4 $mg \cdot mL^{-1}$, 50 mL) was mixed with ammonia solution (450 μL) and hydrazine hydrate (9 μL), and the mixed solution was then stirred at 95 ^{o}C for 1 h. The dispersion was centrifuged for 30 min at 9000 rpm to remove any flocculated aggregate. The final dispersion contained ~0.1 $mg \cdot mL^{-1}$ of reduced graphene.

Horizontally Organized Array of Peptide Nanowires and Graphene Composite (PNWs-G). A FF stock solution was freshly prepared by dissolving the lyophilized FF in HFIP at a

concentration of 100 mg·mL^{-1}. The stock solution was then diluted with a certain concentration of graphene dispersion solution (0.05 mg·mL^{-1}, except where stated otherwise) to a final concentration of 2 mg·mL^{-1}. The diluted solution was dropped on the surface of a clean substrate (40 μL·cm^{-2}) such as a silicon wafer, mica wafer or gold plate, and allowed to dry in oven at 50 ^{o}C to form a horizontally organized array of PNWs-G. Control experiments were carried out under the same conditions using aqueous solutions of different pH to dilute the FF stock solution to prepare the unordered peptide nanowires (PNWs).

Characterization. Scanning electron microscopy (SEM) images were recorded with a Zeiss Supra 55 field emission scanning electron microscope after the samples were coated with a thin layer of platinum. Transmission electron microscopy (TEM) images were obtained on Hitachi H-800 electron microscope with an accelerating voltage of 200 kV to characterize the FF assemblies. The samples were prepared by dropping 10 μL FF–graphene dispersion or FF aqueous solution (2 mg·mL^{-1}) on a carbon-coated copper grid and then dried at 50 ^{o}C. The formed nanowire structure was confirmed by TEM images (Figure S1, Supporting Information). X-ray diffraction (XRD) measurements were performed using a Shimadzu XRD-6000 X-ray diffractometer with Cu Kα radiation (λ = 0.154 nm) at a scan rate of 3° min^{-1}. Fourier transform Infrared (FTIR) spectra were measured on a Bruker Vertex 70 FT-IR spectrometer. Powder samples were obtained by scraping the PNWs-G or PNWs from silicon substrates and mixing with KBr into a disc for the FTIR measurements. UV-vis spectra were recorded on a UV-2501PC spectrophotometer (Shimadzu, Japan). A RF-5301PC spectrofluorometer (Shimadzu, Japan) was used to measure the photoluminescence of peptides in different solutions in a 1.0 cm quartz cuvette. Zeta potential measurements of graphene solutions were performed using a Brookhaven ZetaPlus zeta potential analyzer. Electrochemical impedance spectroscopy measurements were carried out using a CHI 660B electrochemical workstation (CH Instruments, Shanghai Chenhua

Instrument Corp.) in 5 mM $K_3[Fe(CN)_6]/K_4[Fe(CN)_6]$ (1:1) solution with 0.1 M KCl as a supporting electrolyte. A conventional three-electrode system was employed with a modified glassy carbon (GC) electrode as the working electrode, a platinum wire as the counter electrode, and a saturated Ag/AgCl electrode as the reference electrode. The modified electrodes were prepared by dropping 4 μL of FF-graphene mixture solution, or alone FF water solution and graphene solution on the surface of the clean GC electrodes and then dried in air. The corresponding modified electrodes were denoted as the PNWs-G/GC electrode, the PNWs/GC electrode and the G/GC electrode, respectively.

RESULTS AND DISCUSSION

It has previously been shown that FF can be self-assembled into PNTs or PNWs in aqueous solution.[21] These PNWs spread randomly when applied onto a solid surface, and an unordered and uncontrolled network of PNWs was formed (Figures 1a-c). However, we found that when the aqueous solution was replaced with an appropriate concentration (0.05 or 0.1 $mg{\cdot}mL^{-1}$) of an aqueous graphene dispersion, surprisingly high-density, macroscopic-scale organization and interlacement arrays of PNWs-G (Figures 1d–i) were clearly observed by SEM. The size of the organized arrays can even reach millimeter-scale. The diameter of the PNWs ranged from several tens of nanometers to micrometers, but mainly distributed in the range 100–200 nm (Figures 1f and i). This was much smaller than the diameter of PNWs in absence of graphene (Figures 1b and c). The reason may be attributed to the change of some parameters after the introduction of graphene since the dimensions of the self-assembled PNWs were strongly influenced by the ionic strength, pH and medium during the formation of self-assemblies.[22] When the higher concentration of graphene was employed, aggregated graphene sheets uniformly distributed on the PNWs were directly observed in the SEM image of the product (Figure 1i). Furthermore, the

density of the PNWs-G array could be changed by varying the concentration of graphene (Figures 1f and i).

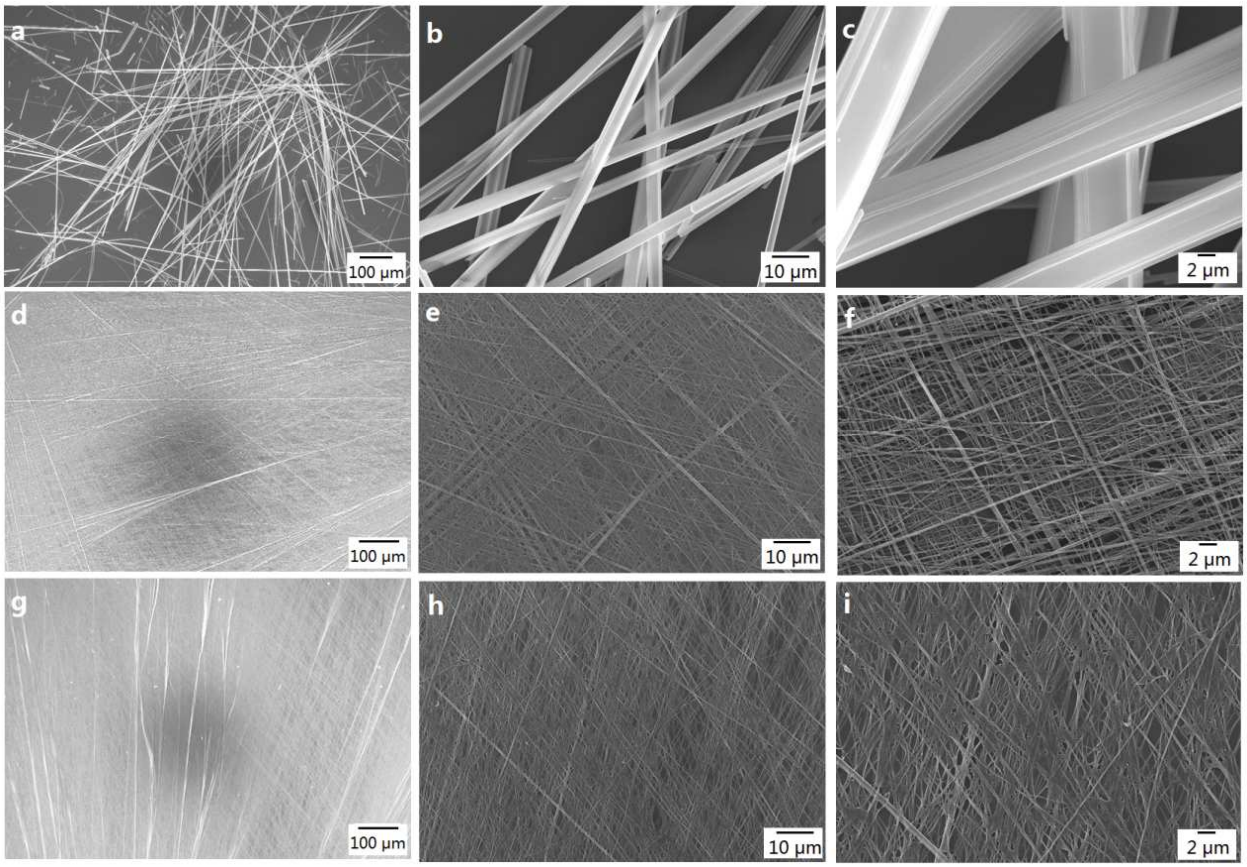

Figure 1. Typical SEM images of the unordered PNWs (a-c) and the organized PNWs-G (d-f for 0.05 and g-i for 0.1 mg mL^{-1} of graphene) on silicon surfaces. From Left to right: low-magnification imaged to high-magnification images. (The black spots in the middle of the a, d and g SEM images were produced by the magnification of the SEM lens being too low.)

The structure of the PNWs-G array was further characterized by XRD and FTIR spectroscopy. Figure 2A shows the XRD patterns of the self-assembled PNWs-G and PNWs on silicon

surfaces. The main diffraction peaks of the PNWs-G were consistent with those of the pure PNWs, and also in agreement with the hexagonal structure previously determined in a study of FF single crystals.[23] Moreover, the FTIR spectra (Figure 2B) of the self-assembled PNWs-G and PNWs both showed a strong peak at 1687 cm^{-1}, which is a characteristic marker band for the β-turn conformation adopted by the molecule.[24,25] No obvious shift between PNWs-G and PNWs was observed from the FTIR spectra. This suggests that FF monomers may be stacked in a β-turn arrangement with hydrogen bonding between the peptides even in the presence of graphene. The close similarities between the XRD patterns and FTIR spectra of the PNWs-G and PNWs lead to

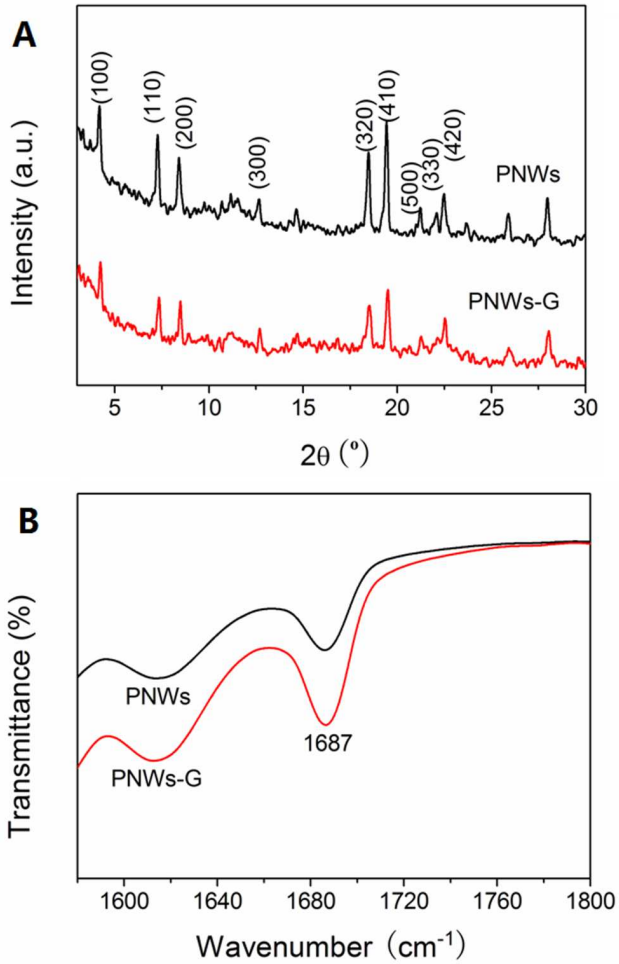

Figure 2. (A) XRD patterns of the PNWs-G and PNWs on silicon surfaces. (B) FTIR spectra of the PNWs-G and PNWs.

the conclusion that the introduction of graphene sheets did not induce any significant changes in the molecular structure or assembly mode of the PNWs.

To understand the action of graphene sheets in the formation of the macroscopic-scale organized nanowire array, the experimental process was closely monitored. When the FF stock solution was added to deionized water, a milky white suspension was immediately observed due to self-assembly of FF into PNTs or PNWs in aqueous solution (Figure S2A left, Supporting Information). In marked contrast, during addition of the FF stock solution to an aqueous graphene dispersion (0.05 $mg{\cdot}mL^{-1}$) a clear solution was observed even when the mixture was left to stand for a few hours (Figure S2A right). To exclude any possibility of the influence of the pH of the graphene dispersion (pH 9.70) on the aggregation process, the FF stock solution was also added to an aqueous solution with the same pH. The result (Figure S2A middle) was similar to that observed in neutral aqueous solution, and an unordered network of PNWs (Figure S2B, Supporting Information) was observed.

The influence of the graphene concentrations on the self–assembly of FF was also studied. When the concentration of graphene was lowered to 0.01 $mg{\cdot}mL^{-1}$, the white suspension (i.e. the self-assembly of FF) could be observed (Figure 3A left) and the corresponding low-density, little interlacement and broad diameters of PNWs were formed (Figure 3B). However, with increasing the concentration to 0.03 $mg{\cdot}mL^{-1}$, the white suspension was hardly seen (Figure 3A second from left). The clear solutions were obtained in the presence of higher concentrations of graphene (Figure 3A third and fourth from left). In order to further probe the phenomena, UV-vis and fluorescence spectra of these solutions in the absence and presence of graphene with different concentrations were measured and shown in Figure S3, Supporting Information. It can be seen that both UV-vis (curve e in Figure S3A) and fluorescence (curve b in Figure S3B) spectra of FF in the presence of 0.05 $mg{\cdot}mL^{-1}$ graphene were different with those of FF in the

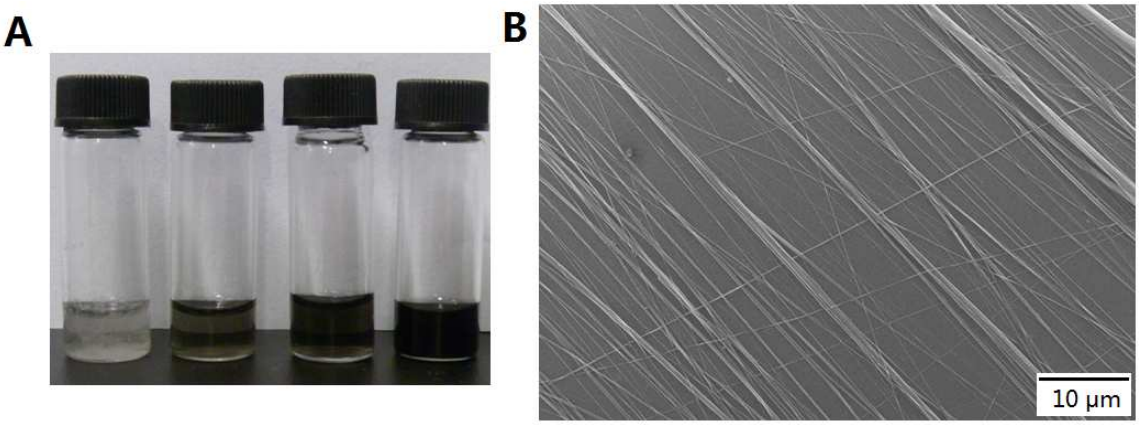

Figure 3. (A) Photographs of mixed peptide solutions, from left to right for aqueous graphene dispersions with concentrations of 0.01, 0.03, 0.05 and 0.1 mg·mL^{-1}. (B) SEM image of PNWs-G on a silicon substrate obtained with a 0.01 mg·mL^{-1} graphene dispersion after drying at 50 ^{o}C.

absence of graphene (curve a in Figure S3A[26] and curve d in Figure S3B). Whereas the spectra of FF in 0.01 mg·mL^{-1} graphene solution (curves c in Figure S3A and S3B) were similar to those of FF in water solution besides the lower intensity of absorption peaks. These spectral characterizations are consistent with the observed phenomena by eyes. The difference of the self-assembly of FF in water solutions and graphene solutions with different concentrations might be attributed to the various amounts of hydrogen bonding and π–π conjugation in these solutions. With increasing the concentration of graphene sheets, the intensity of the absorption at 268 nm increased (curves b, d and f in Figure S3A) and the zeta potential of graphene solutions also enhanced about 7 mV from 0.01 to 0.05 mg·mL^{-1}. These suggest that the higher concentration of graphene could provide more π–π conjugation with the graphene rings and hydrogen bonding with the oxygen functional groups on the surface of graphene sheets. Since the self-assembly of FF monomers involves both hydrogen bonding interactions and π–π stacking of aromatic

residues,[4] the presence of the higher concentration of graphene could interact more strongly on the self-assembly of FF in solutions by the two kinds of acting forces and even might suppress the assembled behavior. These results indicate that the presence of a certain concentration graphene (equal and greater than 0.05 $mg \cdot mL^{-1}$) could play certain parts on the self-assembly of FF in the solution, which finally might result in the formation of the organized PNWs-G array.

After these solutions were deposited on the silicon substrate and the water allowed to be evaporated, the detailed observations by SEM were then followed. As the deposited solution gradually evaporated from the edges to the centre of the substrate, the PNWs grew along the surface of the substrate (Supporting Information, Figure S4). Due to the presence of some graphene sheets on the surface of the substrate, the PNWs may join one another on the surface of graphene sheets and still maintain the same orientation (Figure S1b, Figure 4A and B). These flexible graphene sheets such as nano-'patches' connected the PNWs and "mended" the network (Figure 4c), which finally resulted in the formation of super-long PNWs and a large-scale ordered intertexture of the PNWs on the silicon surface. It is very important for further applications of the organized bionanostructures. In previously reported peptide arrays based on HOPG substrate-directed assembly, the organized arrays could be observed on the nanometer[27] or micron[28] scale, which greatly limited their practical applications. Furthermore, graphene sheets are much cheaper than HOPG. The use of graphene as a template allows the substrate to be varied and the organized self-assembly of peptide nanostructures on gold, glassy carbon and even mica surfaces, as well as silicon, was observed (Supporting Information, Figure S4). These properties make the application of graphite crystal-induced organized bionanostructures more feasible.

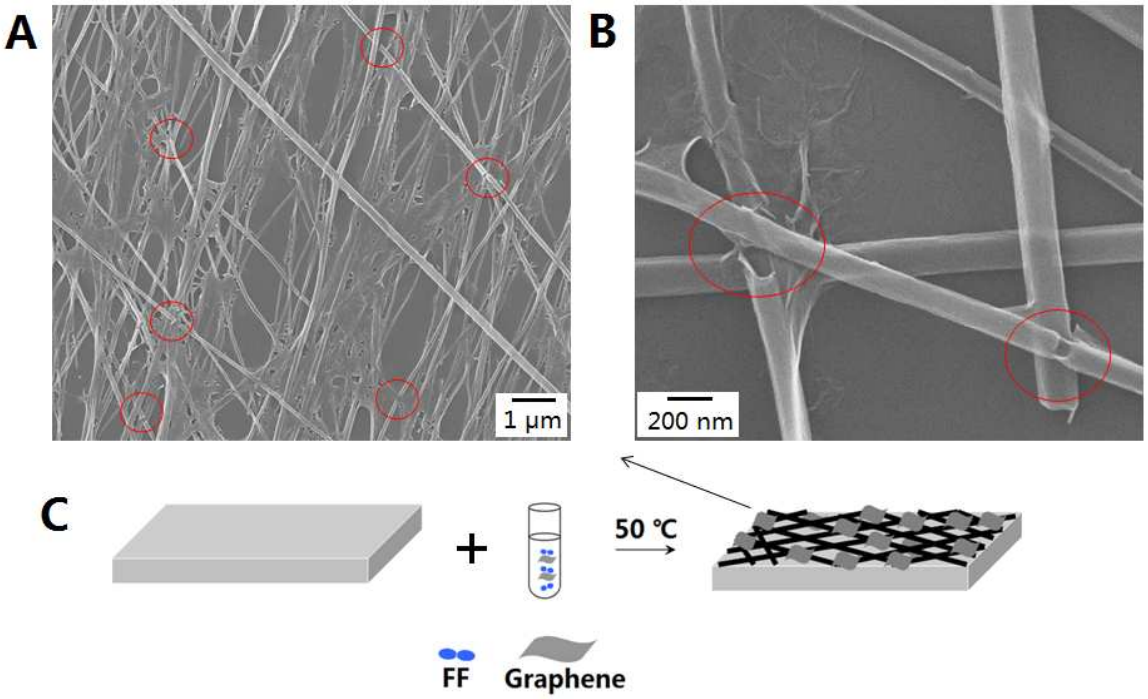

Figure 4. (A, B) The typical SEM images of the PNWs-G on silicon surfaces for 0.05 (A) and 0.1 mg mL^{-1} (B) of graphene dispersion. From these red circle-marks, some PNWs were connected by graphene sheets at the same oriented direction. (C) A schematic illustration of the formation of the macroscopic-scale organized PNWs-G array.

In addition, due to the excellent electrical conductivity of graphene,[29] the introduction of graphene sheets should improve the electronic conductivity of the self-assembled PNWs. This was confirmed by our electrochemical impedance analysis. Figure 5 shows the electrochemical impedance spectra of the PNWs-G and pure PNWs on the surface of glassy carbon (GC) electrodes. The charge transfer resistance (R_{ct}) value for the $Fe(CN)_6^{3-/4-}$ redox probe was measured from the diameter of the semicircle in the Nyquist plots. The value of R_{ct} at the PNWs-G modified electrode was much smaller than that obtained at the PNWs modified electrode, reflecting the much faster electron transfer kinetics at the former electrode. Furthermore, the R_{ct} of the PNWs-G was similar to that of the alone G/GC electrode (Figure S6, Supporting

Information). This may be due to that the presence of PNWs reduced the aggregation of graphene nanosheets during the dry process and facilitated the formation of the interweaving structure, which led to the maintenance of the good electron transfer kinetics even in the presence of PNWs. The enhanced electron-transfer kinetics at the PNWs-G modified electrode is very important for the applications of the peptide nanostructures in electrochemical biosensing,[30,31] bio-inspired energy harvesting devices,[32] and electroactive materials for nerve tissue engineering.[33] In addition, the PNWs-G modified electrode showed the good stability and the current response for the $Fe(CN)_6^{3-}$ maintained 98% of the original response after scanning for 50 cycles.

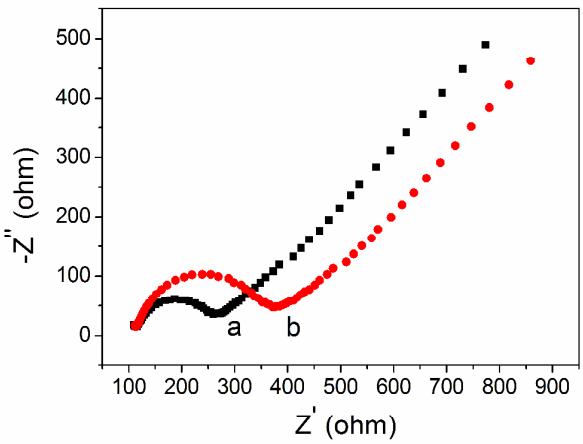

Figure 5. Nyquist plots at the PNWs-G (a) and PNWs (b) on GC electrodes in 5 mM $Fe(CN)_6^{3-/4-}$ containing 0.1 M KCl. The frequency range is from 0.05 Hz to 10 kHz.

The effect of other assembled conditions on the formation of the PNWs-G array was also preliminarily studied. The drying at room temperature (Figure S7, Supporting Information) led to the formation of the low-density and little interlacement array of PNWs-G. According to the previously reported nucleation-driven mechanism of formation for the self-assembly of FF

derived by the vapour–liquid–solid system,[13] the lower nucleation rate and relatively more quick assembled rate of peptides on the surface may be obtained in drying at the relatively lower temperature, which resulted in the formation of large and sparse PNWs. Moreover, the formed PNWs with larger diameters may reduce the interactions with graphene sheets since the two-dimensional sizes of graphene sheets are small. Hence the drying temperature need be controlled for the organized formation of PNWs-G on a solid surface. In addition, the substrates were certainly effective on the density of the formed PNWs-G array (Figure S5, Supporting Information) although the dense and interlaced array of PNWs-G could form on the surface of all these substrates including silicon, gold, glassy carbon and mica. The density of formed PNWs-G array on the mica surface was lowest among these substrates. A possible reason is that mica is more hydrophilic while FF has non-polar aromatic rings, which may lead to lower density of self-assembled peptide nanostructures of similar morphology on the mica surface.[22]

To demonstrate the feature of the organized PNWs-G bionanostructure, an NADH electrochemical sensor based on the PNWs-G modified electrode was further developed as a representative application. The fast and reliable detection of NADH at low potentials is particularly important because NADH is a key component in a whole diversity of dehydrogenase-based bioelectrochemical devices such as biosensors[34,35] and biofuel cells.[36] Figure 6A shows the cyclic voltammetry of the different modified electrodes in pH 7.0 phosphate buffer solution (PBS) containing 1 mM NADH. The PNWs-G/GC electrode exhibited an obvious decrease in overpotential with increasing peak current compared with the bare GC and PNWs/GC electrodes, indicating that the introduction of graphene could effectively improve the electrocatalytic activity toward NADH. It is also noted that the potential of oxidation peak of NADH was located at 0.54 V at the graphene/GC (G/GC) electrode, which was slightly negative relative to the PNWs-G/GC

electrode. Nevertheless, the oxidation current of NADH at the PNWs-G/GC electrode was higher than that at the G/GC electrode.

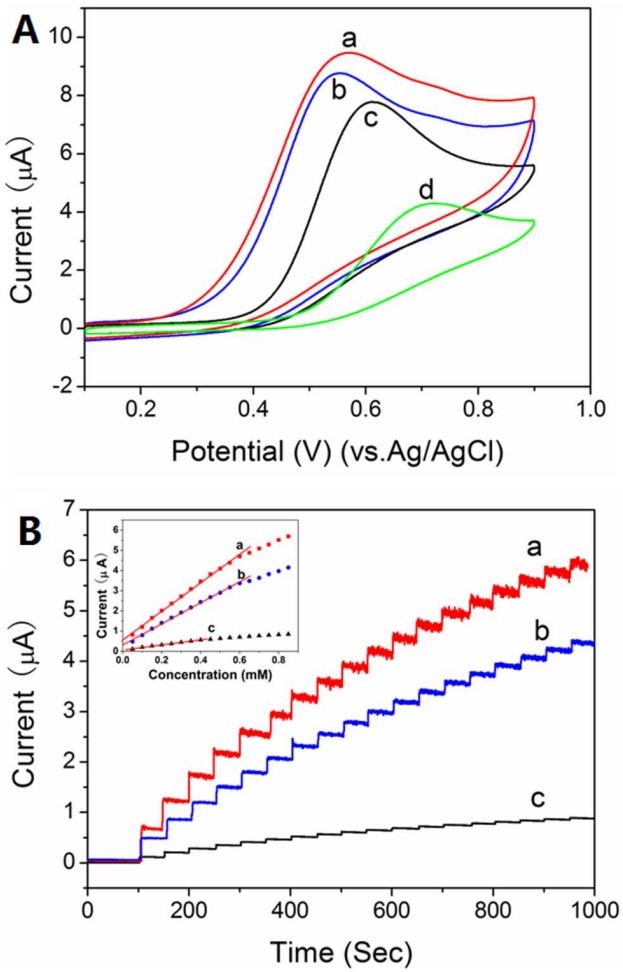

Figure 6. (A) Cyclic voltammograms of the PNWs-G/GC (a), G/GC (b), PNWs/GC (c) and bare GC (d) electrodes in 0.2 M PBS (pH 7.0) containing 1 mM NADH at a scan rate of 50 mV·s^{-1}. (B) Amperometric response curves at the PNWs-G/GC (a), G/GC (b) and PNWs/GC (c) electrodes after successive additions of 50 μM NADH into 0.2 M PBS (pH 7.0) at + 0.5 V. Inset: the corresponding linear calibration plots.

Figure 6B shows the amperometric responses of the different modified electrodes at + 0.50 V to successive additions of 50 μM NADH in 0.2 M PBS (pH 7.0). As expected from the

voltammetric data, the PNWs-G/GC electrode showed a higher current sensitivity of 100.1 nA/μM cm^{-2} for NADH in the linear rang from 50–600 μM (correlation coefficient R^2 = 0.9987), which was more than 5 times larger than that of the PNWs/GC electrode (18.0 nA/μM cm^{-2}, in 50–400 μM, 0.9987) and increased by 35.5% than that of the G/GC electrode (73.8 nA/μM cm^{-2}, in 50–600 μM 0.9983). Also, the PNWs-G/GC electrode showed the lowest detection limit of 1.2 μM (*S/N*=3) among these modified electrodes. Furthermore, the results of the PNWs- G/GC electrode for NADH are much superior to those of previously reported unordered peptide/carbon nanotube nanocomposite/GC electrode (40.37 nA/μM cm^{-2}, 10.0 μM)[37] and chemically reduced graphene oxide/GC electrode (2.68 nA/μM cm^{-2}, 10.0 μM).[38] In addition, four PNWs-G/GC electrodes made independently showed an acceptable reproducibility with a relative standard deviation of 4.2% for the detection of 0.2 mM NADH.

The enhanced sensor performance at the PNWs-G/GC electrode may be attributed to synergistic effects from PNWs and graphene. Introduction of graphene into self-assembled PNWs not only improved the electron transfer reaction of the composite modified electrode, but also led to high density and organized alignment of PNWs on the surface of the electrode. These resulted in the enhanced electrocatalytic responses of the PNWs-G/GC electrode for NADH relative to those of alone peptide nanostructure modified electrode and unordered peptide composite modified electrode.[37] On the other hand, the presence of PNWs reversely reduced the aggregation of graphene nanosheets during the dry process and made the graphene nanosheets uniformly distributed on the surface of the electrode, which also led to the improved performance compared with alone graphene nanosheet modified electrodes.[38] The excellent electrochemical performance of the PNWs-G modified electrode for NADH indicates great promise for the

design of sensitive amperometric biosensors, in connection to the immobilization of suitable dehydrogenase enzymes.

CONCLUSIONS

We develop a simple and mild approach to achieve the formation of a macroscopic-scale, high-density and horizontally organized bionanostructure of PNWs-G on a solid surface by introducing graphene sheets during the self-assembly of FF. The action played by graphene sheets on the formation of the organized PNWs has been explored. Furthermore, due to the incorporation of graphene, the electronic conductivity of the bionanostructure was also significantly improved. In addition, the PNWs-G modified electrode exhibited excellent electrochemical performance toward NADH, suggesting that the PNWs-G bionanostructure has huge potential in sensitive bioelectrochemical devices. The simple and mild approach described here opens a new avenue for the fabrication of macroscopic-scale organized self-assembled peptide bionanostructures on a solid surface, which should be capable to being extended to other biosystems based on graphite surface-template assembly,[27,28,39–41] allowing a variety of functional bionanostructures to be fabricated and used in practical applications.

ASSOCIATED CONTENT

Supporting Information. Typical TEM images of the PNW and PNWs-G; Photograph of a mixed peptide solution in different pH solutions and SEM image of the PNWs formed in pH 9.70 aqueous solution; UV-vis and fluorescence spectra of peptide mixture solution in the absence and presence of graphene sheets with different concentrations; SEM images of the edges of the PNWs-G on silicon surfaces; SEM images of the PNWs-G on gold, mica and glassy carbon

surfaces; Nyquist plots at the G/GC and PNWs-G/GC electrodes; SEM image of the PNWs-G on a silicon substrate in drying at room temperature. This material is available free of charge via the Internet at http://pubs.acs.org.

AUTHOR INFORMATION

Corresponding Author

*E-mail: chenxu@mail.buct.edu.cn.

Notes

The authors declare no competing financial interest.

ACKNOWLEDGMENT

This work was supported by the National Basic Research Program of China (No. 2011CBA00508), the National Natural Science Foundation of China (No. 201175009) and the State Key Laboratory of Electroanalytical Chemistry, CIAC, CAS (No. SKLEAC201203).

REFERENCES

(1) Aggeli, A.; Bell, M.; Boden, N.; Keen, J. N.; Knowles, P. F.; McLeish, T. C. B.; Pitkeathly, M.; Radford, S. E. Responsive Gels Formed by the Spontaneous Self-Assembly of Peptides into Polymeric *β*-Sheet Tapes. *Nature* **1997**, *386*, 259–262.

(2) Hartgerink, J. D.; Beniash, E.; Stupp, S. I. Self-Assembly and Mineralization of Peptide-Amphiphile Nanofibers. *Science* **2001**, *294*, 1684–1688.

(3) Scanlon, S.; Aggeli, A. Self-Assembling Peptide Nanotubes. *Nano Today* **2008**, *3*, 22–30.

(4) Reches, M.; Gazit, E. Casting Metal Nanowires Within Discrete Self-Assembled Peptide Nanotubes. *Science* **2003**, *300*, 625–627.

(5) Ryu, J.; Lim, S. Y.; Park, C. B. Photoluminescent Peptide Nanotubes. *Adv. Mater.* **2009**, *21*, 1577–1581.

(6) Hauser, C. A. E.; Zhang, S. Peptides as Biological Semiconductors. *Nature* **2010**, *468*, 516–517.

(7) Guo, C.; Luo, Y.; Zhou, R. H.; Wei, G. H. Probing the Self-Assembly Mechanism of Diphenylalanine-Based Peptide Nanovesicles and Nanotubes. *ACS Nano* **2012**, *6*, 3907–3918.

(8) Kol, N.; Adler-Abramovich, L.; Barlam, D.; Shneck, R. Z.; Gazit, E.; Rousso, I. Self-Assembled Peptide Nanotubes Are Uniquely Rigid Bioinspired Supramolecular Structures. *Nano Lett.* **2005**, *5*, 1343–1346.

(9) Adler-Abramovich, L.; Reches, M.; Sedman, V. L.; Allen, S.; Tendler, S. J. B.; Gazit, E. Thermal and Chemical Stability of Diphenylalanine Peptide Nanotubes: Implications for Nanotechnological Applications. *Langmuir* **2006**, *22*, 1313–1320.

(10) Yan, X. H.; Zhu, P. L.; Li, J. B. Self-Assembly and Application of Diphenylalanine-Based Nanostructures. *Chem. Soc. Rev.* **2010**, *39*, 1877–1890.

(11) Ryu, J.; Kim, S.-W.; Kang, K.; Park, C. B. Mineralization of Self-Assembled Peptide Nanofibers for Rechargeable Lithium Ion Batteries. *Adv. Mater*. **2010**, *22*, 5537–5541.

(12) Park, B.-W.; Zheng, R.; Ko, K.-A.; Cameron, B. D.; Yoon, D.-Y.; Kim, D.-S. A Novel Glucose Biosensor Using Bi-Enzyme Incorporated with Peptide Nanotubes. *Biosens. Bioelectron.* **2012**, *38*, 295–301.

(13) Reches, M.; Gazit, E. Controlled Patterning of Aligned Self-Assembled Peptide Nanotubes. *Nat. Nanotechnol.* **2006**, *1*, 195–200.

(14) Ryu, J.; Park, C. B. High-Temperature Self-Assembly of Peptides into Vertically Well-aligned Nanowires by Aniline Vapor. *Adv. Mater.* **2008**, *20*, 3754–3758.

(15) Hendler, N.; Sidelman, N.; Reches, M.; Gazit, E.; Rosenberg, Y.; Richter, S. Formation of Well-Organized Self-Assembled Films from Peptide Nanotubes. *Adv. Mater*. **2007**, *19*, 1485–1488.

(16) Adler-Abramovich, L.; Aronov, D.; Beker, P.; Yevnin, M.; Stempler, S.; Buzhansky, L.; Rosenman, G.; Gazit, E. Self-Assembled Arrays of Peptide Nanotubes by Vapour Deposition. *Nat. Nanotechnol*. **2009**, *4*, 849–854.

(17) Hill, R. J. A.; Sedman, V. L.; Allen, S.; Williams, P. M.; Paoli, M.; Adler-Abramovich, L.; Gazit, E.; Eaves, L.; Tendler, S. J. B. Alignment of Aromatic Peptide Tubes in Strong Magnetic Fields. *Adv. Mater*. **2007**, *19*, 4474–4479.

(18) Adler-Abramovich, L.; Gazit, E. Controlled Patterning of Peptide Nanotubes and Nanospheres Using Inkjet Printing Technology. *J. Pept. Sci.* **2008**, *14*, 217–223.

(19) Kovtyukhova, N. I.; Ollivier, P. J.; Martin, B. R.; Mallouk, T. E.; Chizhik, S. A.; Buzaneva, E. V.; Gorchinskiy, A. D. Layer-by-Layer Assembly of Ultrathin Composite Films from Micron-Sized Graphite Oxide Sheets and Polycations. *Chem. Mater.* **1999**, *11*, 771–778.

(20) Li, D.; Müller, M. B.; Gilje, S.; Kaner, R. B.; Wallace, G. G. Processable Aqueous Dispersions of Graphene Nanosheets. *Nat. Nanotechnol.* **2008**, *3*, 101−105.

(21) Kim, J.; Han, T. H.; Kim,Y.-I.; Park, J. S.; Choi, J.; Churchill, D. G.; Kim, S. O.; Ihee, H. Role of Water in Directing Diphenylalanine Assembly into Nanotubes and Nanowires. *Adv. Mater.* **2010**, *22*, 583−587.

(22) Kumaraswamy, P.; Lakshmanan, R.; Sethuraman, S.; Krishnan, U. M. Self-Assembly of Peptides: Influence of Substrate, pH and Medium on the Formation of Supramolecular Assemblies. *Soft Mater* **2011**, *7*, 2744−2754.

(23) Görbitz, C. H. Nanotube Formation by Hydrophobic Dipeptides. *Chem. Eur. J.* **2001**, *7*, 5153−5159.

(24) Gupta, M.; Bagaria, A.; Mishra, A.; Mathur, P.; Basu, A.; Ramakumar, S.; Chauhan, V. S. Self-Assembly of A Dipeptide-Containing Conformationally Restricted Dehydrophenylalanine Residue to Form Ordered Nanotubes. *Adv. Mater.* **2007**, *19*, 858−861.

(25) Yan, X. H.; Cui, Y.; He, Q.; Wang, K. W.; Li, J. B. Organogels Based on Self-Assembly of Diphenylalanine Peptide and their Application to Immobilize Quantum Dots. *Chem. Mater.* **2008**, *20*, 1522−1526.

(26) Amdursky, N.; Molotskii, M.; Gazit, E.; Rosenman, G. Elementary Building Blocks of Self-Assembled Peptide Nanotubes. *J. Am. Chem. Soc.* **2010**, *132*, 15632−15636.

(27) Kowalewski, T.; Holtzman, D. M. In Situ Atomic Force Microscopy Study of Alzheimer's β–amyloid Peptide on Different Substrates: New Insights into Mechanism of β-Sheet Formation. *Proc. Natl. Acad. Sci. USA* **1999**, *96*, 3688−3693.

(28) Brown, C. L.; Aksay, I. A.; Saville, D. A.; Hecht, M. H. Template-Directed Assembly of A *De Novo* Designed Protein. *J. Am. Chem. Soc.* **2002**, *124*, 6846–6848.

(29) Rao, C. N. R.; Sood, A. K.; Subrahmanyam, K. S.; Govindaraj, A. Graphene: The New Two-Dimensional Nanomaterial. *Angew. Chem., Int. Ed.* **2009**, *48*, 7752–7777.

(30) Yemini, M.; Reches, M.; Gazit, E.; Rishpon, J. Peptide Nanotube-Modified Electrodes for Enzyme–Biosensor Applications. *Anal. Chem.* **2005**, *77*, 5155–5159.

(31) Oliverira, I. D. O.; Alves, W. A. Electrochemical Determination of Dopamine Based on Self-Assembled Peptide Nanostructure. *ACS Appl. Mater. Interfaces* **2011**, *3*, 4437–4443.

(32) Kholkin, A.; Amdursky, N.; Bdikin, I.; Gazit, E.; Rosenman, G. Strong Piezoelectricity in Bioinspired Peptide Nanotubes. *ACS Nano* **2010**, *4*, 610–614.

(33) Zelzer, M.; Ulijn, R. V. Next-Generation Peptide Nanomaterials: Molecular Networks, Interfaces and Supramolecular Functionality. *Chem. Soc. Rev.* **2010**, *39*, 3351–3357.

(34) Radoi, A.; Compagnone, D. Recent Advanced in NADH Electrochemical Sensing Design. *Bioelectrochemistry* **2009**, *76*, 126–134.

(35) Kachoosangi, R. T. K.; Musameh, M. M.; Abu-Yousef, I.; Yousef, J. M.; Kanan, S. M.; Xiao, L.; Davies, S. G.; Russell, A.; Compton, R. G. Carbon Nanotube-Ionic Liquid Composite Sensors and Biosensors. *Anal. Chem.* **2009**, *81*, 435–442.

(36) Yan, Y.; Zheng, W.; Su, L.; Mao, L. Carbon-Nanotube-Based Glucose/O_2 Biofuel Cells. *Adv. Mater.* **2006**, *18*, 2639–2643.

(37) Yuan, J. H.; Chen, J. R.; Wu, X. H.; Fang, K. M.; Niu, L. A NADH Biosensor Based on Diphenylalanine Peptide/Carbon Nanotube Nanocomposite. *J. Electroanal. Chem.* **2011**, *656*, 120−124.

(38) Zhou, M.; Zhai, Y.; Dong, S. Electrochemical Sensing and Biosensing Platform Based on Chemically Reduced Graphene Oxide, *Anal. Chem.* **2009**, *81*, 5603−5613.

(39) Yang, G. C.; Woodhouse, K. A.; Yip, C. M. Substrate-Facilitated Assembly of Elastin-Like Peptides: Studies by Variable-Temperature in Situ Atomic Force Microscopy. *J. Am. Chem. Soc.* **2002**, *124*, 10648−10649.

(40) Yu, X.; Wang, Q. M.; Lin, Y. N.; Zhao, J.; Zhao, C.; Zheng, J. Structure, Orientation, and Surface Interaction of Alzheimer Amyloid-β Peptides on the Graphite. *Langmuir* **2012**, *28*, 6595−6605.

(41) So, C. R.; Hayamizu, Y.; Yazici, H.; Gresswell, C.; Khatayevich, D.; Tamerler, C.; Sarikaya, M. Controlling Self-Assembly of Engineered Peptides on Graphite by Rational Mutation. *ACS Nano* **2012**, *6*, 1648−1656.

TOC Graphic